Indian Journal of Chemistry
Vol. 65, February 2026, pp. 82-90
DOI: 10.56042/ijc.v65i2.18004

Synthesis, characterization and catalytic application of a coordination compound of cobalt(II) based on 2,6-pydc and TMDP for degradation of dyes under dark

Aieshri Swargiary[a], Tanmoy Kumar Ghosh[b], Anamika Kalita Deka[a] & Arunendu Mondal*[a]

[a] Department of Chemistry, Central Institute of Technology Kokrajhar (Deemed to University under Ministry of Education, Govt. of India), Kokrajhar 783 370, Assam, India

[b] Department of Chemistry, University College of Science, University of Calcutta, Kolkata 700 009, India
E-mail: a.mondal@cit.ac.in

Received 18 March 2025; accepted (revised) 29 January 2026

A cobalt(II) coordination polymer of 2,6-pyridinedicarboxylic (2,6-pydc) and 4,4′-trimethylenedipyridine (4,4′-TMDP) has been resynthesized by a new synthetic method. The polymer is then characterized through single crystal XRD (SC-XRD) analysis. Variety of other techniques such as elemental analysis, TGA, fluorescence spectroscopy, UV-Vis spectroscopy, FTIR spectroscopy and magnetic study have been employed for further characterization. This coordination polymer has been explored as a catalyst for degradation of methyl orange (MO) and congo red (CR) in an aqueous medium with the reducing agent sodium borohydride ($NaBH_4$) under dark. Surprisingly, it is observed that 96.41% and 97.22% degradation of MO and CR dyes occurs within 8 and 10 minutes with rate constants 0.491 min^{-1} and 0.264 min^{-1} respectively.

Keywords: 4,4′-Trimethylenedipyridine, 2,6-Pyridinedicarboxylic acid, Methyl orange, Congo red

The increasing population in the last few decades has resulted in a proliferation of industries, which includes textiles, dyeing, leather, paper and plastic production. These industries utilize various colorizing agents to enhance the appearance of a wide range of products. However, the discharge of waste materials from these sectors into aquatic environments leads to water pollution, posing threats to both aquatic ecosystems and human beings[1,2]. The colorizing agents involved are often resistant to natural degradation due to their complex organic compositions[3]. Among these, anionic dyes (methyl orange, MO and congo red, CR) are particularly significant as major contributors to water pollution[4]. The disposal of these dyes into water bodies severely impacts aquatic life and can subsequently introduce toxicity to humans through the food chain, thereby causing a range of health-related problems[4,5]. Various methodologies have been implemented for the treatment of waste water prior to its discharge into water bodies[6]. Techniques such as adsorption[7], Fenton reaction[8], photocatalysis[9] and reductive degradation[10] have been explored by diverse researchers for the remediation of dyes in the presence of nanoparticles. Recent studies have also documented the photocatalytic degradation of MO and CR utilizing composite materials[11,12] and metal-coordinated compounds[1,13,14]. Nevertheless, there exists paucity of research regarding the degradation of dyes under dark conditions, with limited studies having addressed this phenomenon[12,15]. Synthesis of polymeric coordination compounds of different dimensions(1D, 2D, 3D) with various carboxylic acid-substituted pyridine ligands has been well documented in the literature[16–25]. These compounds have demonstrated their usefulness across multiple applications such as catalysis[26–28], gas storage and separation[29,30], water harvesting[31], antibacterial activity[32,33], *etc*. In this study, an unique coordination polymer of cobalt(II) $[\{Co(TMDP)(H_2O)_4\}_n\{Co(2,6\text{-}pydc)_2\}]\cdot H_2O$, composed of a cationic polymer and anionic monomer has been explored as catalyst for the degradation of these dyes and surprisingly it shows very promising result.

Experimental sections

Materials

$Co(NO_3)_2.6H_2O$ is taken from Fischer Scientific. TMDP and 2,6-pydc are taken from Hi media laboratories. $NaBH_4$ is taken from Emplura. The dyes MO and CR are taken from Loba Chemie Pvt. Ltd and Merck Life Science Private Limited. All the chemicals are used directly without further purification.

Synthesis of [{Co(TMDP)$(H_2O)_4$}$_n${Co(2,6-pydc)$_2$}]·H_2O (1)

Aqueous solution of mixture of TMDP (1 mmol, 0.198g), 2,6-pydc (1mmol, 0.167g) and $Co(NO_3)_2.6H_2O$ (1mmol, 0.291g) is placed in an autoclave and heated in an oven at 100°C for about 24hrs. After cooling at RT, it is filtered and red-brown crystals are collected. Although, the synthesis of the similar compound has been reported earlier,[34] the synthesis process is different from the reported one. Yield: 60% (0.392g). Analytical. Calcd for $C_{27}H_{32}Co_2N_4O_{14}$: C, 42.94; N, 7.42; H, 4.24. Found: C, 42.51; N, 7.62; H, 4.80%.

Characterization techniques

BRUKER D8 VENTURE SC-XRD is used to collect single crystal data using dual X-ray sources (Mo-Kα). BRUKER D8 ADVANCE is used to collect powder XRD data using X-ray source (Cu K-alpha). Shimadzu FTIR 8201 spectrophotometer is used to collect FTIR spectroscopy data using KBr pellet in the range of 4000 to 400cm^{-1}. Shimadzu UV-2600 UV-Vis spectrophotometer is used to collect UV-Visible data in solid state using $BaSO_4$ as standard reference. EuroEA elemental analyser (model Eurovector EA3000) is used for elemental analysis. SII 6300 EXSTAR thermogravimetric analyser is used to collect thermal analysis data (heating rate of 10°C/min) in N_2 atmosphere. Magnetic behaviour is studied by vibrating sample magnetometer (VSM, model: 7410 series) and Agilent (Varian) Cary Eclipse spectrophotometer is used to collect fluorescence spectrum.

X-ray crystallographic data collection and refinement

The collection of the crystallographic data of compound **1** is carried out with BRUKER D8 VENTURE SC-XRD using dual X-ray sources (Mo-Kα). The structure is solved by direct methods and refined by full-matrix least squares on F^2 using the SHELXL2018/3 package and Olex2 program[35,36]. The SADABS program is used to carry out the absorption corrections[37]. The cell parameters and other crystallographic data are similar to that of the reported one[34].

Catalytic activity

The resynthesized polymeric compound of cobalt(II) is applied as catalyst for degradation of MO and CR with $NaBH_4$. MO (1×10^{-4}M), CR (1×10^{-4}M) and $NaBH_4$ (0.1M) are prepared separately by dissolving in distilled water. The catalytic activities are performed under dark at RT. The reaction is started by adding 20 mL of MO and 20 mL of freshly prepared $NaBH_4$ in a round bottomed flask followed by addition of 60 mL of distill water. Then 25mg of the catalyst is added to the reaction mixture. The disappearance of colour is monitored with UV-Vis spectrophotometer at regular intervals by collecting the solution in 3.5 mL cuvette. Similar procedure is also applied to study the degradation of CR in presence of the catalyst.

Results and Discussion

Single crystal XRD analysis (SC-XRD)

The compound **1** is analyzed by SC-XRD. The crystal system is found to be monoclinic with space group *P2/*c; the cell parameters of the crystal structure are a = 9.7591(6)Å, b= 8.9652(5)Å and c=18.2578(11)Å with α = γ =90° and β=99.400° respectively which are in accordance with the reported one[34]. The crystal structure of the compound **1** is shown in Fig. 1. The crystallographic study reveals that the crystal structure of the

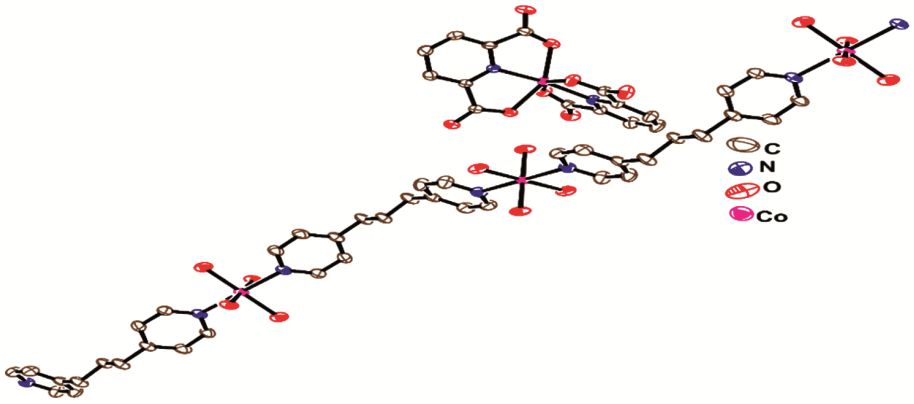

Fig. 1 — ORTEP view of [{Co(TMDP)$(H_2O)_4$}$_n${Co(2,6-pydc)$_2$}]·H_2O (**1**). The hydrogen atoms and solvent water molecule are omitted for clarity

compound consists of two separate cationic and anionic moieties. The cationic part is polymer whereas the anionic part is a monomer. In the polymeric part, TMDP acts as a bridging ligand connected two cobalt atoms and each cobalt atom is coordinated by four water molecules. In this polymeric structure the Co-N bond length is found to be 2.2513(12)Å. On the other hand, in the monomeric part the cobalt atom is coordinated by two 2,6-pydc ligands. Two oxygen atoms of two different COO^- groups and one nitrogen atom of each 2,6-pydc is coordinated to cobalt atom. In the monomeric structure the Co-N bond length is found to be 2.0400(10)Å. The selected bond lengths and bond angles are given in Table 1 and Table 2.

X-ray powder diffraction study (PXRD)

X-ray powder diffraction study of the synthesized compound **1** is used to confirm the single phase of the bulk material. Fig. 2 is the comparison of experimental powder pattern with that of stimulated powder pattern from X-ray single crystal data. The major peaks of the experimental PXRD pattern of the bulk material in Fig. 2(a) matches with the stimulated one in Fig. 2(b). This confirms that the synthesized bulk compound **1** is in same phase. The structure is also same as determined by single crystal X-ray study.

Table 1 — Selected bond lengths of $[\{Co(TMDP)(H_2O)_4\}_n\{Co(2,6\text{-}pydc)_2\}]\cdot H_2O$ (**1**)

	Bond lengths (Å)
Co(1)–O(1)	2.1502(10)
Cu(1)–O(2)	2.1813(11)
Co(1)–N(1)	2.0400(10)
Co(2)–O(5)	2.0531(9)
Co(2)–O(6)	2.0943(11)
Co(2)–N(2)	2.2513(12)

Fourier transform infrared spectroscopy (FTIR)

Fig. S1 is the FTIR spectrum of compound **1,** which resembles with the reported one. The broad peak centered at 3252 cm^{-1} is for the presence of water molecules[38] in the crystal. The peaks at 1078 cm^{-1} and 1010 cm^{-1} are for C – O and C – C respectively[39]. The weak peak at 503 cm^{-1} is for Co – O stretching vibrations[39]. The peaks at 1614 cm^{-1} and 1379 cm^{-1} are for asymmetric and symmetric stretching vibrations of COO^- respectively[40]. The weak peak at 1282 cm^{-1} is due to C – N stretching vibration[41].

UV-Visible spectroscopy (UV-Vis)

The solid-state UV-Visible spectrum of the compound **1** is recorded at RT within the range of 200 – 850 nm. In the UV-Visible spectrum of the compound **1** (Fig. S2) the bands observe at 231 nm and 259 nm are due to $\pi - \pi^*$ transitions[42]. The band observe at 349 nm is mainly for the ligand-to-metal charge transfer transitions of the compound[43].

Thermogravimetric analysis (TGA)

Fig. 3 is the TGA pattern of the compound **1** within the temperature range of 35 – 650°C at 10°C/min heating rate. In the first step within the temperature 98°C to 162 °C five water molecules get dissociated with weight loss of 13% (calc. 12%). Then the compound **1** shows stability upto 219°C which confirms the thermal stability of the dehydrated compound and after that again decomposition continues. In the second step it may be assumed that one molecule of 2,6-pydc get dissociated with weight

Table 2 — Selected bond angles of $[\{Co(TMDP)(H_2O)_4\}_n\{Co(2,6\text{-}pydc)_2\}]\cdot H_2O$ (**1**)

	Bond angles (°)		Bond angles (°)
O(1)–Co(1)–O(2)	151.34(4)	O(5)–Co(2)–O(5)[b]	180.00
O(1)–Co(1)–O(1)[a]	97.66(4)	O(5)–Co(2)–O(6)[b]	86.06(4)
O(1)–Co(1)–O(2)[a]	87.29(4)	O(5)–Co(2)–N(2)[b]	88.52(4)
O(1)–Co(1)–N(1)	75.80(4)	O(6)–Co(2)–N(2)	91.05(4)
O(1)–Co(1)–N(1)[a]	94.67(4)	O(6)–Co(2)–O(6)[b]	180.00
N(1)–Co(1)–N(1)[a]	165.70(5)	O(6)–Co(2)–N(2)[c]	88.95(4)
O(2)–Co(1)–N(1)	75.67(4)	N(2)–Co(2)–N(2)[c]	180.00
O(2)–Co(1)–O(2)[a]	101.81(4)	–	–
O(2)[a]–Co(1)–N(1)[a]	113.86(4)	–	–
O(2)[a]–Co(1)–N(1)	75.67(4)	–	–
O(5)–Co(2)–O(6)	93.94(4)	–	–
O(5)–Co(2)–N(2)	91.48(4)	–	–

[a] = 1-x,y,3/2-z, [b] = 1-x,1-y,1-z

loss of 22.97% (calc. 22.15%) followed by loss of remaining volatile components at high temperature.

Fluorescence spectroscopy

Fig. S3 is the fluorescence spectra of the compound **1** and parent ligands 2,6-pydc and TMDP taken at RT in DMF solution. The ligands show high intensity bands centered at 349nm. The bands may be due to n - π* / π - π* transition[44]. The compound **1** shows a much lower intensity centered at 349nm than the parent ligands. The lower intensity of the compound **1** may be due to partially filled d orbital of the cobalt ion which led to ligand to metal charge transfer (LMCT)[44]. The similarity of the spectral position of the ligands and the compound **1** in the same wavelength suggest that the fluorescence of compound **1** is mainly due to proposed transition within the ligands.

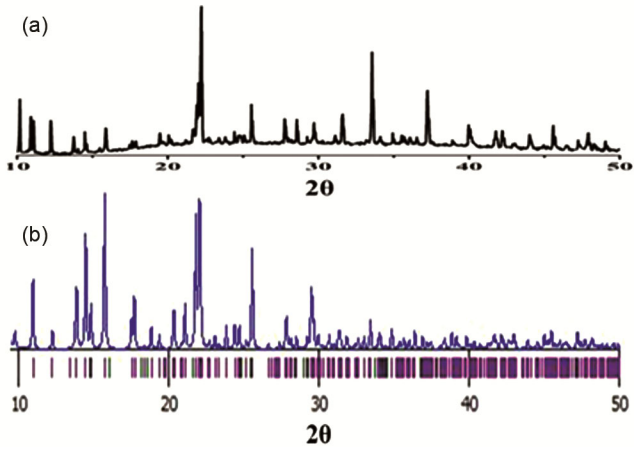

Fig. 2 — (a) Experimental PXRD pattern of bulk [{Co(TMDP)$(H_2O)_4$}$_n${Co(2,6-pydc)$_2$}]·H_2O (**1**) (b) Stimulated PXRD pattern of [{Co(TMDP)$(H_2O)_4$}$_n${Co(2,6-pydc)$_2$}]·H_2O (**1**)

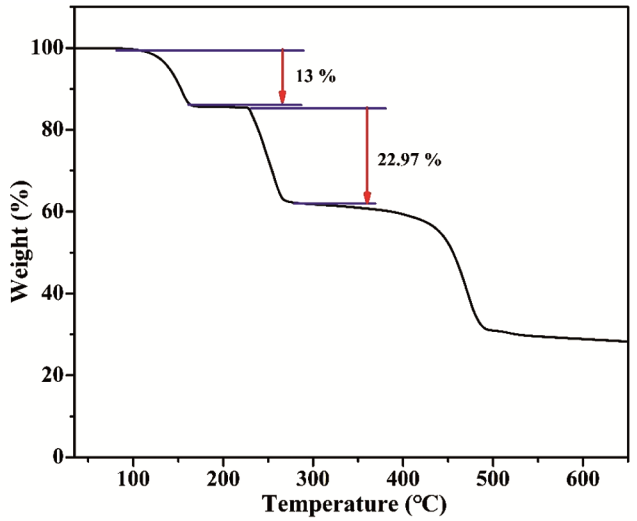

Fig. 3 — TGA curve of [{Co(TMDP)$(H_2O)_4$}$_n${Co(2,6-pydc)$_2$}]·H_2O (**1**)

Optical band gap energy (E_g)

The band gap energy of the compound **1** is determined by Tauc formula using the equation 1.

$$(\alpha h\upsilon)^n = C(h\upsilon - E_g) \quad \ldots(1)$$

where α indicates the absorption coefficient, generally calculated as α = (2.303×absorption)/t, "t" indicates the cuvette thickness (1cm), "C" indicates a constant, "E_g" indicates the band gap energy, n indicates the exponent that depends on the transition type and h indicates the Planck's constant. Fig. 4 is the plot of $(\alpha h\upsilon)^2$ *vs* hυ. The band gap energy is found to be 4.04 eV indicating as semiconducting material[45]. This high band gap is also an indication that the compound **1** may not be a good candidate for photocatalytic study.

Magnetic analysis

Fig. S4 is the magnetic hysteresis loop of the compound **1**, measured by vibrating sample magnetometer at RT. The magnetic saturation (Ms), remanent magnetization (Mr) and coercieve force (Hc) values are found to be 45.34 emu/g, 4.46 emu/g and 122.30 Oe respectively. The value of Ms is found to be higher than Hc, indicating ferromagnetic behaviour of the compound **1**[31].

Catalytic study for the reductive degradation of MO and CR

The degradation of MO and CR with reducing agent $NaBH_4$ are done at RT in presence of cobalt(II) compound as catalyst. The dyes solutions are collected at different intervals of time and

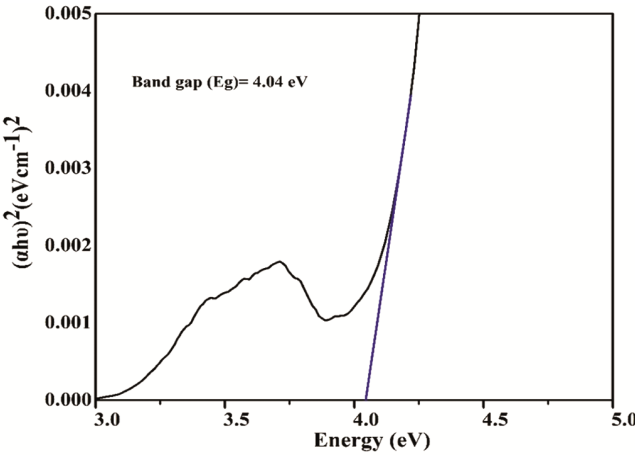

Fig. 4 — Band gap energy of [{Co(TMDP)$(H_2O)_4$}$_n${Co(2,6-pydc)$_2$}]·H_2O (**1**)

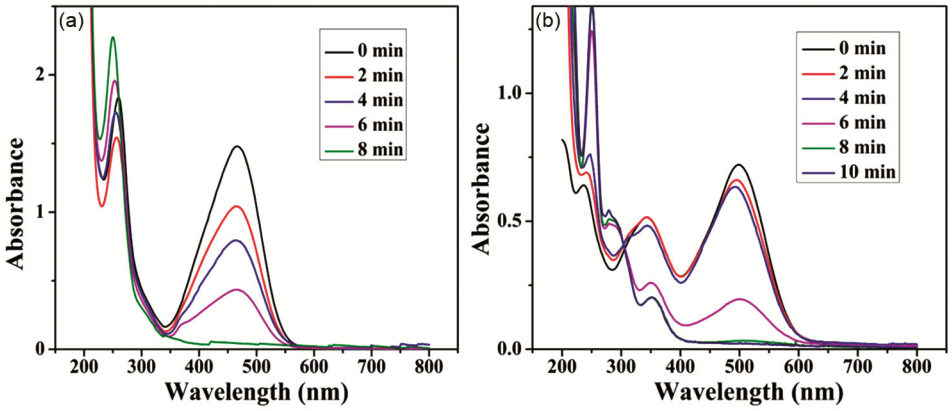

Fig. 5 — Catalytic degradation of (a) MO and (b) CR with $NaBH_4$

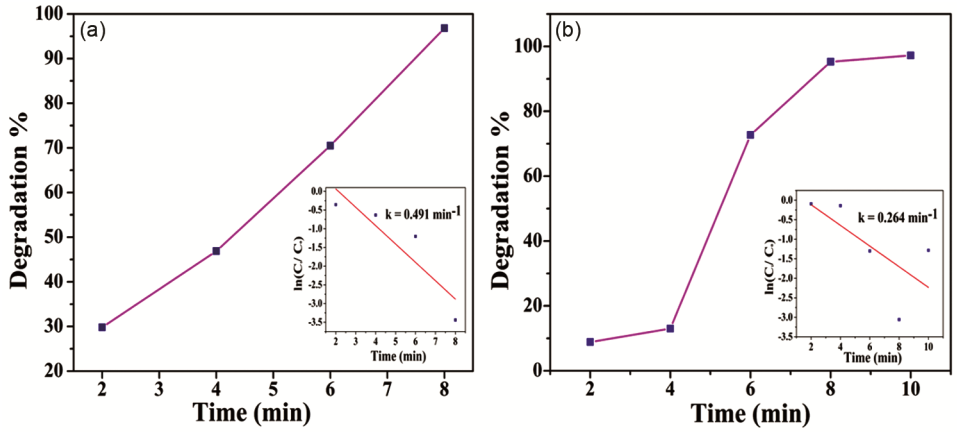

Fig. 6 — Degradation % *vs* time graph of (a) MO [inset ln (C_t/C_o) *vs* time plot] and (b) CR [inset ln (C_t/C_o) *vs* time plot]

simultaneously the absorbances are monitored with UV-Visible spectrophotometer. The UV-Visible spectra of catalytic degradation of MO and CR dyes are depicted in Fig. 5. MO and CR show strong absorbance peaks at 467nm and 497nm respectively. The decrease in intensity at 467nm and 497nm for MO and CR indicates the reduction of azo groups (-N=N-) for both the dyes. As per the literature report the reductive degradation of MO leads to the formation of two new compounds, sulphanilic acid and *p*-phenyl diamine[46,47]. The discoloration of the dyes is also confirmed by the appearance of new peaks at 249nm for MO and 345nm as well as 249nm for CR[48]. The degradation percentage, which is depicted in Fig. 6 are calculated using equation 2[49,50].

$$\text{Degradation \%} = \{(C_o - C_t)/ C_o\} \times 100 \quad \ldots(2)$$

Rate of degradation is monitored by measuring the variation in color of the dyes with respect to the reaction time. The rate of the reaction follows the first order kinetics which is confirmed by the equation 3 (Ref. 51).

$$\ln (C_t/C_o) = -k \times t \quad \ldots(3)$$

where, "$\mathbf{C_o}$" is the initial concentation of the dye solution and "$\mathbf{C_t}$" is the the concentration of the dye solution after time t, "**k**" is rate constant and "**x**" is the indication of the multiplication sign.

The degradation percentage are found to be 96.41% for MO and 97.22% for CR respectively. The rate of degradation of the dyes has been predicted by studying the reduction kinetics, indicating pseudo first order reaction. The linear correlation plot of ln (C_t/C_o) *vs* time (t) is shown in Fig. 6 (inset). The rate constants (k) for MO and CR degradation are found to be 0.491min^{-1} and 0.264min^{-1} respectively. The degradation of MO and CR with $NaBH_4$ without the catalyst are also studied (Fig. 7). The study reveals that the MO dye takes much longer time to degrade completely and CR dye remains stable for a very longer period of time without degradation in absence of catalyst.

Comparative study

Table 3 and Table 4 are the comparative study of MO and CR degradation in the presence of the

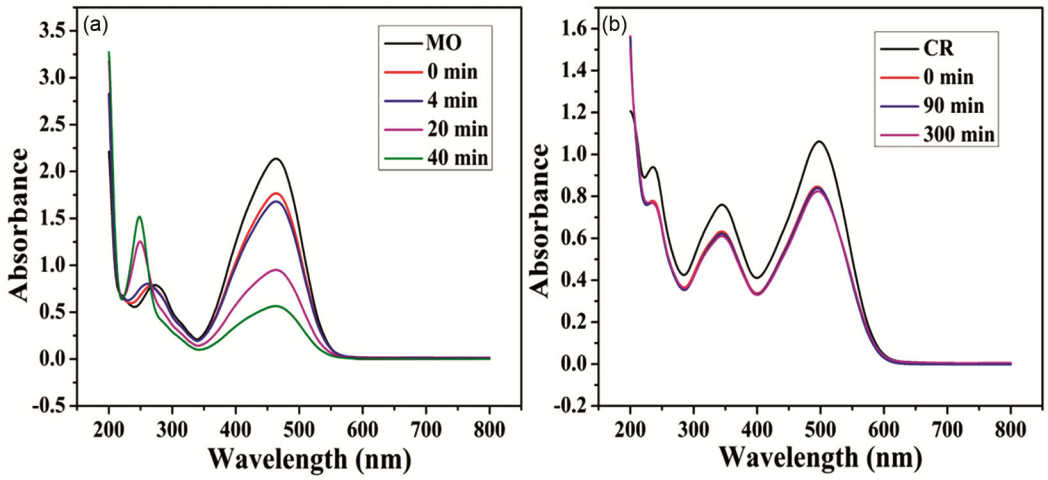

Fig. 7 — Degradation of (a) MO and (b) CR with $NaBH_4$ in absence of catalyst

Table 3 — Comparison of catalytic degradation of MO

Sl. No	Compd / composite material	Time (min)	Degradation %	Condition	Reference
1	$[\{Co(TMDP)(H_2O)_4\}_n\{Co(2,6\text{-}pydc)_2\}]\cdot H_2O$ (**1**)	8	96.41	Dark	This study
2	$[\{Cu(TMDP)(2,3\text{-}pydc)\}\cdot 2H_2O]_n$	60	97	Dark	Swargiary *et al.*[53]
3	$[Co(2,6\text{-}pydc)(bibp)_{0.5}(H_2O)_2]_n$	120	79.4	Light	Zhang *et al.*[1]
4	$[Ni(2,6\text{-}pydc)(bibp)_{0.5}(H_2O)_2]_n$	120	78.5	Light	Zhang *et al.*[1]
5	$[Co(2,6\text{-}pydc)(bbibp)_{1.5}]_n$	120	81.3	Light	Zhang *et al.*[1]
6	$[Ni(2,6\text{-}pydc)(bbibp)_{1.5}]_n$	120	77.4	Light	Zhang *et al.*[1]
7	$[Zn(2,6\text{-}pydc)(bbibp)_{0.5}]_n$	120	46.9	Light	Zhang *et al.*[1]
8	Cd(bpyp)(nba)	9	35.44	Light	Zhao *et al.*[52]
9	[Cu(MPBMPA)Cl] (ClO_4)	90	100	Light	Carvalho *et al.*[54]
10	[Cu(PABMPA)Cl]Cl	60	100	Light	Carvalho *et al.*[54]
11	$[Cu(PBMPA)]ClO_4$	60	100	Light	Carvalho *et al.*[54]
12	$[Cu(BMPA)Cl_2]$	60	100	Light	Carvalho *et al.*[54]
13	$MnTiO_3$perovskite	180	79.4	Light	Kitchamsetti *et al.*[11]
14	Nano-$LaMnO_3$	280	90	Dark	Rekavandi *et al.*[12]
15	Nano-$LaMnO_3$	60	100	Solar	Rekavandi *et al.*[12]
16	$\{[Pb(Tab)_2(bpe)]_2(PF_6)_4\}_n$	300	95	Light	Wang *et al.*[14]
17	Perovskite –type $LaNiO_3$	360	86.6	Dark	Zhong *et al.*[15]

Table 4 — Comparison of catalytic degradation of CR

Sl. No	Compd / composite material	Time (min)	Degradation %	Condition	Reference
1	$[\{Co(TMDP)(H_2O)_4\}_n\{Co(2,6\text{-}pydc)_2\}]\cdot H_2O$ (**1**)	10	97.22	Dark	This study
2	$[\{Cu(TMDP)(2,3\text{-}pydc)\}\cdot 2H_2O]_n$	240	76	Dark	Swargiary *et al.*[53]
3	$MnTiO_3$perovskite	180	79.4	Light	Kitchamsetti *et al.*[11]
4	$\{[Cd_2(H_2O)_2(tpeb)_2(1,2\text{-}CHDC)_2]\cdot H_2O\}_n$	90	90	Light	Zhang *et al.*[13]
5	$[Cu(BMPA)Cl_2]$	90	88	Light	Carvalho *et al.*[54]

synthesized catalyst with that of the reported coordination compounds and composite materials. The literature review shows that till date among the coordination compounds and composite materials for MO dye degradation, Cd(bpyp)(nba)[52] is the fastest one and it helps to degrade only 35.44% within 9 minutes. Comparative study with the coordination compound **1** reveals its performance as catalyst is even better than Cd(bpyp)(nba)[52], where it achieved 96.41% degradation of MO within just 8 minutes. On

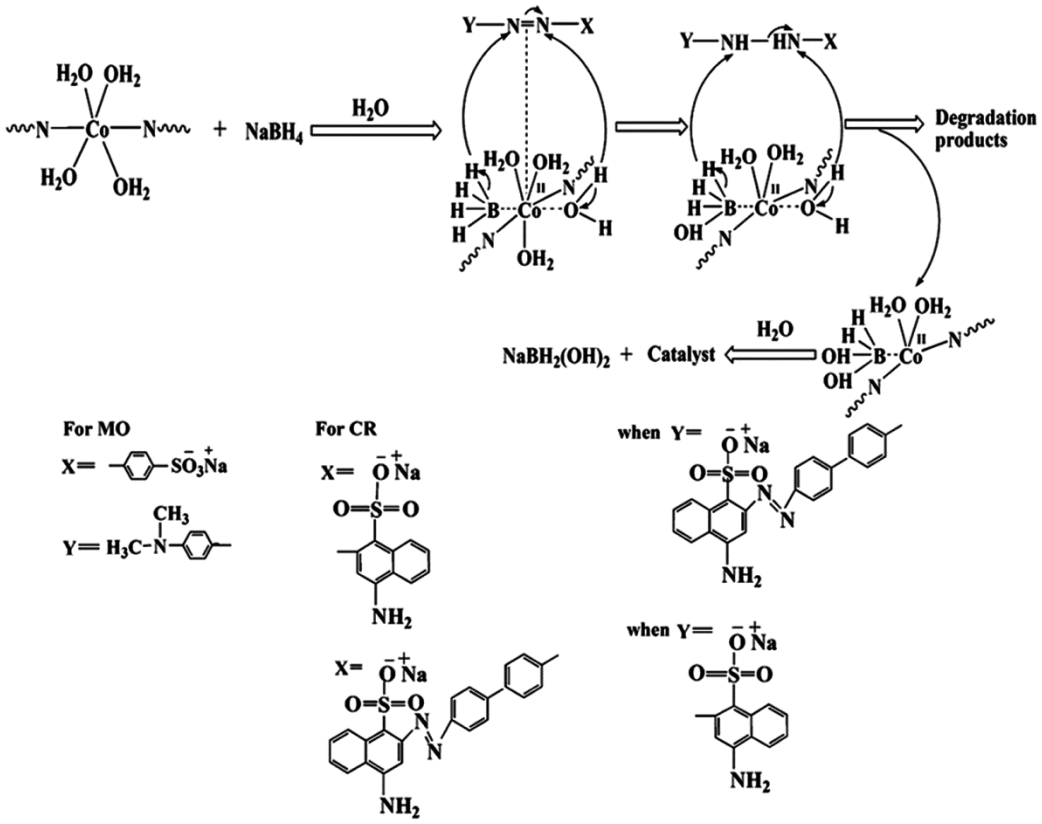

Scheme 1 — Probable mechanism for degradation

the other hand, the performance of compound **1** as catalyst for dye degradation of CR with $NaBH_4$ is much superior than other materials as catalyst (Table 4). Remarkably, 97.22% degradation within only 10 minutes under dark has been achieved which is far better than $\{[Cd_2(H_2O)_2(tpeb)_2(1,2\text{-}CHDC)_2]\cdot H_2O\}_n$[13] (90% degradation within 90 minutes under light). This comparative study reveals, compound **1** emerged as a far better candidate as catalyst for degradation of both MO and CR dyes.

Degradation mechanism

Freshly prepared $NaBH_4$ solution is added to the catalyst to form $NaBH_2(OH)_2$ and as a result the catalyst along with $NaBH_4$ enables the degradation of MO. Scheme 1 is the probable degradation mechanism of MO. Similar type of mechanism has been reported in the literature[6,53]. First one hydride ion from BH_4^- species and one H^+ from the coordinated water molecule, reduce the —N=N— group to imine. Again, another hydride ion from BH_4^- species and one H^+ from the coordinated water molecule reduce the imine group to amine. The final products after degradation are assumed to be sulphanilic acid (p-aminobenzenesulphonilic acid) and the p-phenyldiamine. The absorption peaks in the UV-Visible spectrum at 467nm shows decrease with increase in time along with formation of new peaks at 249nm: mainly attributed to the sulphanilic acid as reported[55].

Reductive degradation of CR also follows the same mechanism. The two —N=N— groups are reduced to imines by attacking two hydride ions from two BH_4^- and two H^+ from two coordinated water molecules. Later, the two imine groups are further reduced to amines by attacking another two hydride ions from two BH_4^- and two H^+ from two coordinated water molecules. As the literature reported[56], two molecules of 3,4-diamino-1-naphthalenesulphonic acid and one molecule of biphenyldiamine are assumed to produce after degradation.

Conclusions

A coordination compound of cobalt(II), $[\{Co(TMDP)(H_2O)_4\}_n\{Co(2,6\text{-}pydc)_2\}]\cdot H_2O$ (**1**) has been successfully resynthesized using hydrothermal method, which is different from reported one and it has been characterized through various analytical

techniques. It is to be noted that the higher optical band gap value (4.04 eV), is indicative that the compound **1** may not act as a photocatalysts for degradation of dyes since photocatalytic degradation usually occurs with lower band gap value. Performance of **1** as a catalyst for degradation of MO and CR with reducing agent $NaBH_4$ under dark conditions at RT was remarkable. When compared with other reported data in terms of percentage degradation and time taken, this catalyst achieved a milestone of 96.41% and 97.22% within 8 minutes and 10 minutes for MO and CR respectively.

Supplementary Information

Supplementary information is available in the website https://nopr.niscpr.res.in/handle/123456789/58776.

Acknowledgements

The authors are thankful to NECBH (IIT Guwahati), IIT Roorkee, Guwahati Biotech Park, SAIF Gauhati University and CIT Kokrajhar for their help and support throughout the work. Aieshri Swargiary also acknowledges BTC, Kokrajhar, Assam, India for financial support to carry out the research.

References

1 Zhang D M, Xu C G, Liu Y Z, Fan C B, Zhu B & Fan Y H, *J Sol State Chem*, 290 (2020) 121549.
2 Pereira L & Alves M, *Environmental Protection Strategies for Sustainable Development,* (Springer, Dordrecht), 2012, p. 111.
3 Zhu Z S, Qu J, Hao S M, Han S, Jia K L &Yu Z Z, *ACS Appl Mat Int*, 10 (2018) 30670.
4 Zainudin N F, Sam S T, Wong Y S, Ismail H, Walli S, Inoue K, Kawamura G & Tan W K, *Polymers*, 15 (2023) 237.
5 Solano A M S, Garcia-Segura S, Martínez-Huitle C A & Brillas E, *Appl Catal B: Env*, 168–169 (2015) 559.
6 Mondal A, Adhikary B & Mukherjee D, *Coll Surf A: Physicochem Eng Asp*, 482 (2015) 248.
7 Goudarzi M, Bazarganipour M & Salavati-Niasari M, *RSC Adv*, 4 (2014) 46517.
8 Nidheesh P V, Gandhimathi R & Ramesh S T, *Env Sci Poll Res*, 20 (2013) 2099.
9 Singla P, Sharma M, Pandey O P & Singh K, *Appl Phys A: Mat Sci Proc*, 116 (2014) 371.
10 Bokare A D, Chikate R C, Rode C V & Paknikar K M, *Appl Cat B: Env*, 79 (2008) 270.
11 Kitchamsetti N, Didwal P N, Mulani S R, Patil M S & Devan R S, *Heliyon*, 7 (2021) e07297.
12 Rekavandi N, Malekzadeh A & Ghiasi E, *Nanochem Res*, 4 (2019) 1.
13 Zhang J G, Gong W J, Guan Y S, Li H X, Young D J & Lang J P, *Cryst Growth Des*, 18 (2018) 6172.
14 Wang F, Li F L, Xu M M, Yu H, Zhang J G, Xia H T & Lang J P, *J Mat Chem A*, 3 (2015) 5908.
15 Zhong W, Jiang T, Dang Y, He J, Chen S -Y, Kuo C -H, Kriz D, Meng Y, Meguerdichian A & Suib S L, *Appl Catal A Gen*, 549 (2018) 302.
16 Zhou X, Guo X, Liu L, Shi Z, Pang Y & Tai X, *Crystals,* 9 (2019) 166.
17 Wang L, Du H, Wang Y, Wang M & Tian Z, *Integr Ferroelectr*, 200 (2019) 199.
18 Yan S, Li X & Zheng X, *J Mol Struc*, 929 (2009) 105.
19 Yin H & Liu S-X, *J Mol Struc*, 918 (2009) 165.
20 Barszcz B, Hodorowicz M, Jabłonska-Wawrzycka A, Masternak J, Nitek W & Stadnicka K, *Polyhedron*, 29 (2010) 1191.
21 Yin W-X, Liu Y-T, Ding Y-J, Lin Q, Lin X-M, Wu C-L, Yao X-D & Cai Y-P, *Cryst Eng Comm*, 17 (2015) 3619.
22 Patrick B O, Stevens C L, Storr A & Thompson R C, *Polyhedron*, 22 (2003) 3025.
23 Rafizadeh M, Amani V & Tayebee R, *Bull Chem Soc Ethiop*, 22 (2008) 93.
24 Vasquez-Ríos M G, Rojas-León I, Montes- Tolentino P, Hernández-Ahuactzi I F & Höpfl H, *Cry Growth Des*, 18 (2018) 7132.
25 Terenti N, Ferbinteanu M & Lazarescu A, *Chem J Mold*, 13 (2018) 24.
26 Li Z, Liu Y-Y, Xu G-H & Ma J-F, *Polyhedron*, 178 (2020) 114324.
27 Bu F-X, Hu M, Xu L, Meng Q, Mao G-Y, Jiang D-M & Jiang J-S, *Chem Comm*, 50 (2014) 8543.
28 Loukopoulos E & Kostakis G E, *J Coord Chem*, 71 (2018) 371.
29 Jiaqi Y, Li J, Kan L, Zou L, Zhao J, Li D, Li G, Zhang L-R & Liu Y, *Cryst Growth Des*, 18 (2018) 5449.
30 Hiraide S, Sakanaka Y, Kajiro H, Kawaguchi S, Miyahara M T & Tanaka H, *Nat Comm*, 11 (2020) 3867.
31 Xu W & Yaghi O M, *ACS Cent Sci*, 6 (2020) 1348.
32 Yan L, Gopal A, Kashif S, Hazelton P, Lan M, Zhong W & Chen X, *Chem Eng J*, 435 (2022) 134975.
33 Yu X-Y, Zhang R, Li S-L, Yu S-H, Gao L, Yan W-F, Jin J & Luo Y-N, *Inorg Chem Comm*, 116 (2020) 107897.
34 Islam S, Dey P & Seth S K, *Polyhedron*, 242 (2023) 116514.
35 Dolomanov O V, Bourhis L J, Gildea R J, Howard J A K & Puschmann H, *J Appl Cryst*, 42 (2009) 339.
36 Sheldrick G M, *Acta Crystallogr. Sect. A: Found. Crystallogr*, 64 (2008) 112.
37 SAINT and SADABS versions 6.02 and 2.03 2002 Bruker AXS Inc.: Madison, WI.
38 Sanotra S, Gupta R, Sheikh H N, Kalsotra B L, Gupta V K & Rajnikant, *Monatsh Chem*, 144 (2013) 1807.
39 Zang Q, Zhong G Q & Wang M L, *Polyhedron*, 100 (2015) 223.
40 Tella A C, Oladipo A C, Adimula V O, Olayemi V T, Dembaremba T O, Ogunlaja A S, Clarkson G J & Walton R I, *Polyhedron*, 192 (2020).
41 Ucar I, Karabulut B, Bulut A & Buyukgungor O, *J Mol Struct*, 834–836 (2007) 336.
42 Yenikaya C, Poyraz M, Sarı M, Demirci F, Ilkimen H & Buyukgungor O, *Polyhedron* 28 (2009) 3526.
43 Jin J, Gong Y, Li L, Han X, Meng Q, Liu Y & Niu S, *Spectrochim Acta Part A: Mol Biomol Spect*, 137 (2015) 856.
44 Chen S-Y, Sun H-X, Guo Y-C & Cao F-P, *Asian J Chem*, 25 (2013) 3134.
45 Ghosh M K, Pathak S & Ghorai T K, *ACS Omega*, 4 (2019) 16068.
46 Nguyen T T-N, Vo T-T, Nguyen B N-H, Nguyen D-T, Dang V-S, Dang C-H & Nguyen T-D, *Env Sci Poll Res*, 25 (2018) 34247.

47 Joseph S & Mathew B, *Mater Sci Eng B*, 195 (2015) 90.
48 Sha Y, Mathew I, Cui Q, Clay M, Gao F, Zhang X J & Gu Z, *Chemosphere*, 144 (2016) 1530.
49 Mathur M, Gola D, Panja R, Malik A & Ahammad S Z, *Env Sci Poll Res*, 25 (2018) 345.
50 Gola D, kriti A, Bhatt N, Bajpai M, Singh A, Arya A, Chauhan N, Srivastava S K, Tyagi P K & Agrawal Y, *Curr Res Green Sust Chem*, 4 (2021)100132.
51 David L & Moldovan B, *Nanomaterials*, 10 (2020) 202.
52 Zhao J, Dang Z, Muddassir M, Raza S, Zhong A, Wang X & Jin J, *Molecules*, 28 (2023) 6848.
53 Swargiary A, Ghosh T K & Mondal A, *J Chem Sci*, 136 (2024)
54 Carvalho S S F, Rodrigues A C C, Lima J F & Carvalho N M F, *Inorg Chim Acta*, 512 (2020) 119924.
55 Fan J, Guo Y, Wang J & Fan M, *J Hazard Mater*, 166 (2009) 904.
56 Naz M, Rafiq A, Ikram M, Haider A, Ahmad S O A, Haider J & Naz S, *J Mat Sci*, 56 (2021) 15572.